Preparation and Photoluminescent Characterization of Poly(phenylene vinylene)/TiO_2 Nanoparticles Composite Nanofibers by One-Step Electrospinning

Yang Xie,[1] Liguo Sun,[1] Cheng Wang,[1] Shuhong Wang,[1] Guoqiang Xu,[1] Jian Zhang,[2] Eryun Yan[3]

[1]*Key Laboratory of Polymer Functional Materials, School of Chemistry and Materials Science, Heilongjiang University, Harbin, 150080, People's Republic of China*
[2]*Group Information Center, BASF SE, Ludwigshafen, D-67056, Germany*
[3]*College of Material Science and Engineering, Qiqihar University, Qiqihar, 161006, People's Republic of China*

Received 8 November 2011; accepted 28 November 2011
DOI 10.1002/app.36618
Published online in Wiley Online Library (wileyonlinelibrary.com).

ABSTRACT: A simple electrospinning progress, directly mixing method, was used to produce ultrafine poly(phenylene vinylene)/TiO_2 (PPV/TiO_2) composite nanofibers with diameters ranging from 100 to 300 nm. The effects of different TiO_2 content on diameter, morphology, and structure of composite fibers were analyzed by scanning electron microscopy and transmission electron microscope. The results showed that composite polymer nanofibers with smooth surface were obtained when TiO_2 concentration was below 18 wt %. The surface of the composite nanofibers became rougher with the increase of TiO_2 content. The optical properties of the as-prepared nanofibers were characterized by photoluminescence spectra and photographs, the results showed an increase in intensity of the high-energy shoulder (510 nm) when the concentration of nanoparticles increased. X-ray diffraction measurements showed that the increasing TiO_2 content enhanced the amorphous phase of PPV in composite nanofibers. © 2012 Wiley Periodicals, Inc. J Appl Polym Sci 000: 000–000, 2012

Key words: composites; nanofibers; morphology; luminescence

INTRODUCTION

In recent years, dimensionally modulated materials with integrated platform of nanostructured materials are highly desirable for advanced nanoscaled electronic and optoelectronic applications.[1] As an electrostatic fiber fabrication technique, electrospinning has attracted much interest due to its versatility and potential for applications in diverse fields.[2] During electrospinning, the key phenomenon of "bending instability" elongates the electrospinning jet up to 100,000 times in terms of milliseconds.[3] This phenomenon results in an extremely large elongational flow rate, which can closely align macromolecular chains along the nanofiber axis. Incorporation of optoelectronically active materials such as conjugated polymers and nanoparticles into electrospun nanofibers is an appealing method to study their optical and electronic properties and to fabricate optoelectronic devices at the nanometer scale.[4]

Poly(phenylene vinylene) (PPV) as conjugated polymer are important candidate for polymer optoelectronic devices due to its excellent photo- and electroluminescence (PL and EL), photovoltaic (PV), and nonlinear optical properties as well as its easily processing and low cost.[5,6] Up to now, many articles have reported that a feasible way to improve the optoelectronic properties is to combine PPV and its derivatives with nanoparticles or (and) other polymer, such as enhancing PL-efficiency in PPV/ZnO,[7] MPN-PPV/CdSe,[8] tunable fluorescence color in CdS/PPV/PVA,[9] CdTe/PPV/PVA,[10] improving PV behaviors in PPV/Pt,[11] and MEH-PPV/CdS[12] nanocomposite. The reason is: the interaction was occurred between conjugated polymer and semiconductor nanoparticles, such as energy transfer or

Correspondence to: C. Wang (wangc_93@yahoo.com).
Contract grant sponsor: NSFC; contract grant numbers: 20872030, 21072049, 21074031.
Contract grant sponsor: CPDF; contract grant number: 201104428.
Contract grant sponsor: NSF of Heilongjiang; contract grant numbers: E201118, E201144.
Contract grant sponsor: Abroad Person with Ability Foundation of Heilongjiang Province; contract grant numbers: 1251G070, 11551339, 11541273, 11551335, 2010td03.
Contract grant sponsor: Innovation Fellowship Foundation of Heilongjiang University; contract grant number: Hdtd2010-11.

TABLE I
The Denotation and Composition of PPV/TiO_2 Mixed Solutions (g)

Sample denotation	PPV precursor (4.5 wt %)	TiO_2	Ethanol	TiO_2 : PPV
PPV	4.5002	0.0000	4.5	0 : 100
PPV/TiO_2 1	4.5003	0.0161	4.5	8 : 100
PPV/TiO_2 2	4.5000	0.0245	4.5	12 : 100
PPV/TiO_2 3	4.5001	0.0365	4.5	18 : 100
PPV/TiO_2 4	4.4998	0.0487	4.5	24 : 100
PPV/TiO_2 5	4.5003	0.0916	4.5	45 : 100

charge transfer, which enhance photoelectric properties of composite materials.[7]

Polymer/inorganic nanocomposites are usually prepared by sol–gel process,[13–15] *in situ* synthesis,[16] directly mixing one-step method,[17] and so on. Comparing with these methods, the directly mixing electrospinning is not only relatively simple but also has the advantage of producing composite nanofibers at a high speed and low cost. Using the one-step electrospinning method provides opportunities to obtain ultrafine polymer/inorganic composite fibers, which combine the advantages of polymer/inorganic hybrids and large-surface area nanofibers together, and meet the need of new materials.[18] Among all the inorganic particles, TiO_2 is one of the most extensively studied because of its remarkable optical and electronic properties.[19]

On the basis of the research mentioned above, we synthesized TiO_2 nanoparticles and fabricated PPV/TiO_2 hybrid nanofibers by electrospinning technique. The composite nanofibers with excellent fluorescent properties are potentially interesting for many applications such as micro- and nano-optoelectronic devices and systems.

EXPERIMENTAL

Materials

Tetrahydrothiophene and *p*-xylylene dichloride were purchased from Tokyo Chemical Industry Limited Company. Tetrabutyl titanate ($Ti(OC_4H_9)_4$), acetone, and ethanol were obtained from Tianjin Fuyu Chemical Limited Company. All chemicals and solvents were used without further purification.

Preparation of electrospinning solutions

The PPV precursor was prepared according to Wessling's synthetic route[20] and the optimized conditions provided by Halliday et al.[21] Precursor aqueous solution was dialyzed in water for a week, and then it was placed in a ventilated place for a week to remove the water fully. As a result, the thick solution of PPV (4.5 wt %) precursor was obtained.

The TiO_2 nanoparticles were prepared by hydrolysis of precipitation of titanium alkoxide.[21] The synthesized TiO_2 nanoparticles were centrifugalized and washed repeatedly with deionized water and dispersed ultrasonically in ethanol to form suspensions. Ethanol-soluble TiO_2 nanoparticles were mixed with the PPV precursor in different mass ratios and the mixtures were vigorously stirred for at least 3 h at room temperature and ultrasonically treated for 10 min before electrospinning. The denotation and composition of PPV/TiO_2 mixed solutions was shown in Table I.

Electrospinning process

The electrospinning setup used in this study consisted of a 10-mL syringe with a needle (IDZ, 0.8 mm), an aluminum collecting plate, and a high voltage supply. The PPV precursor/TiO_2 nanoparticles spinning solutions were electrospun at a positive voltage of 12 kV and a working distance of 25 cm (the distance between the needle tip and the collecting plate). The solution was continuously supplied using a syringe pump at a rate of 0.5 mL/h. All the electrospinning procedures were carried out at room temperature. The aluminum foils with nanofibers were heated at 120°C under nitrogen for 15 min to remove the residual solvents and then heated at 220°C for conversion of the precursor to PPV.

Characterization

The morphology of the PPV/TiO_2 composite nanofibers was studied by field-emission scanning

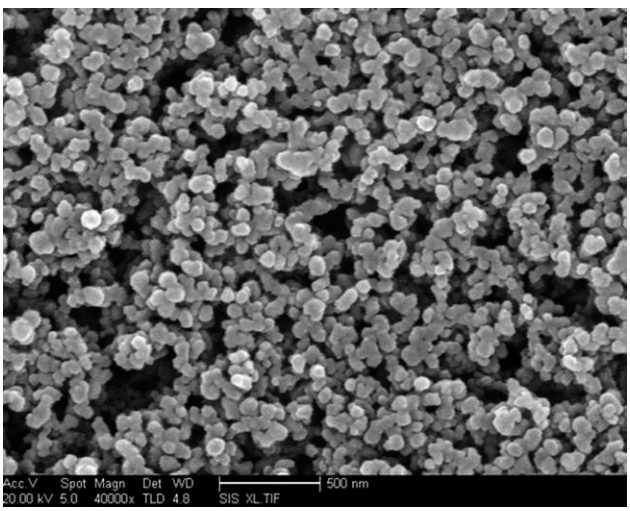

Figure 1 SEM image of the as-prepared TiO_2 nanoparticles.

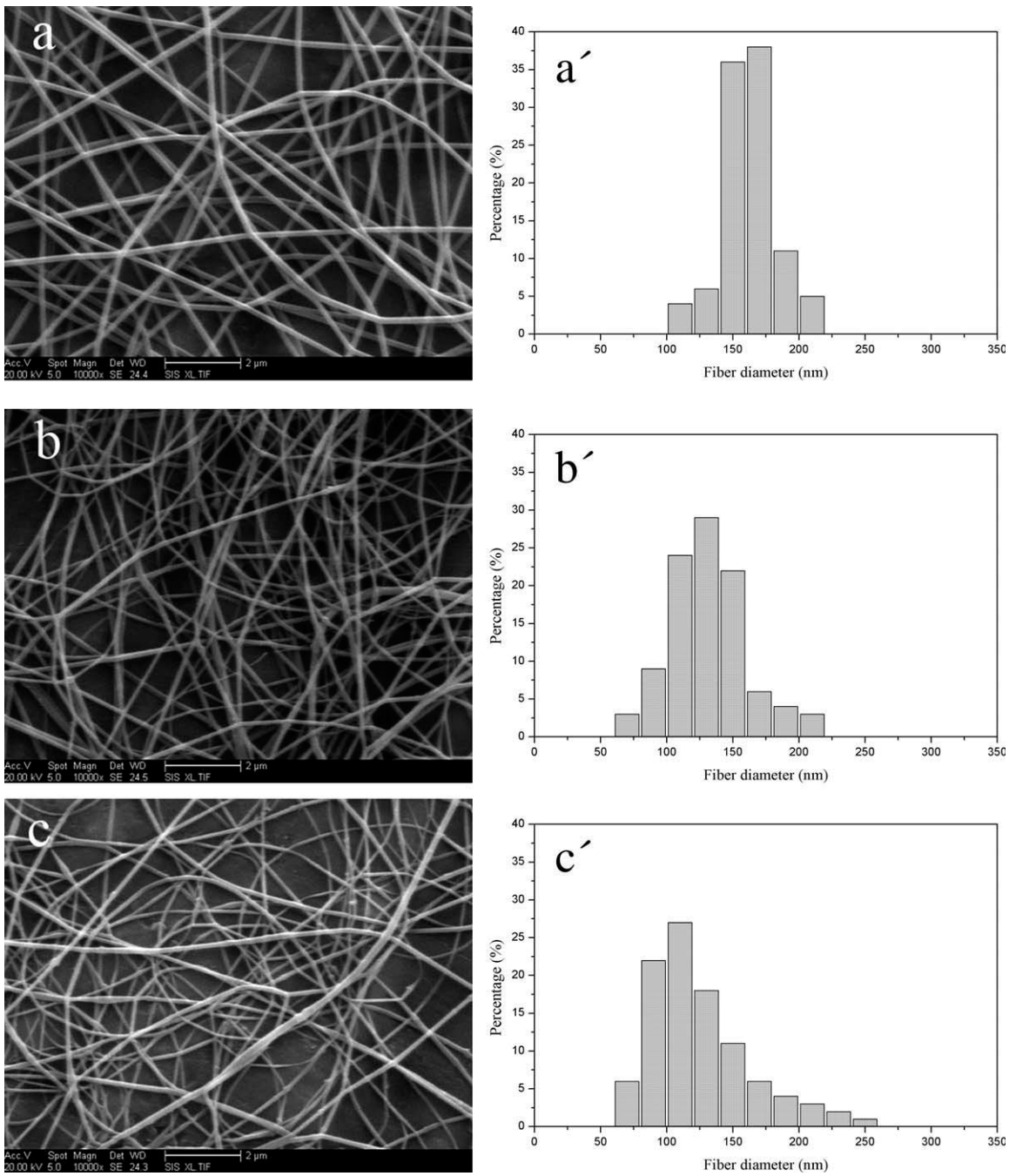

Figure 2 SEM images of the electrospun PPV/TiO_2 composite nanofibers with various TiO_2 contents: (a) 0 wt %, (b) 8 wt %, (c) 12 wt %, (d) 18 wt %, (e) 24 wt % and (f) 45 wt %, and the corresponding diameter distribution (a′), (b′), (c′), (d′), (e′), (f′).

electron microscopy (FE-SEM, MX2600FE) and transmission electron microscope (TEM, FEI TECNAI F20). The average nanofibers diameter (AFD) was determined from the FE-SEM images and around 50 nanofibers were analyzed. The samples were prepared by collecting the nanofibers on copper grids coated with a layer of amorphous carbon. The electrical conductivity of the spinning solutions was measured by conductivity meter (DDS-307). A combined stead state fluorescence and phosphorescence lifetime spectrometer (FLSP920) was used to obtain the PL spectra of the as-spun nanofibers and the excitation wavelength was 470 nm. The fluorescent images of nanofibers were taken from a fluorescence microscopy (TE2000-U). X-ray diffraction (XRD) (D8 advance) studies were performed to investigate the crystallinity of TiO_2 nanoparticles and composite nanofibers.

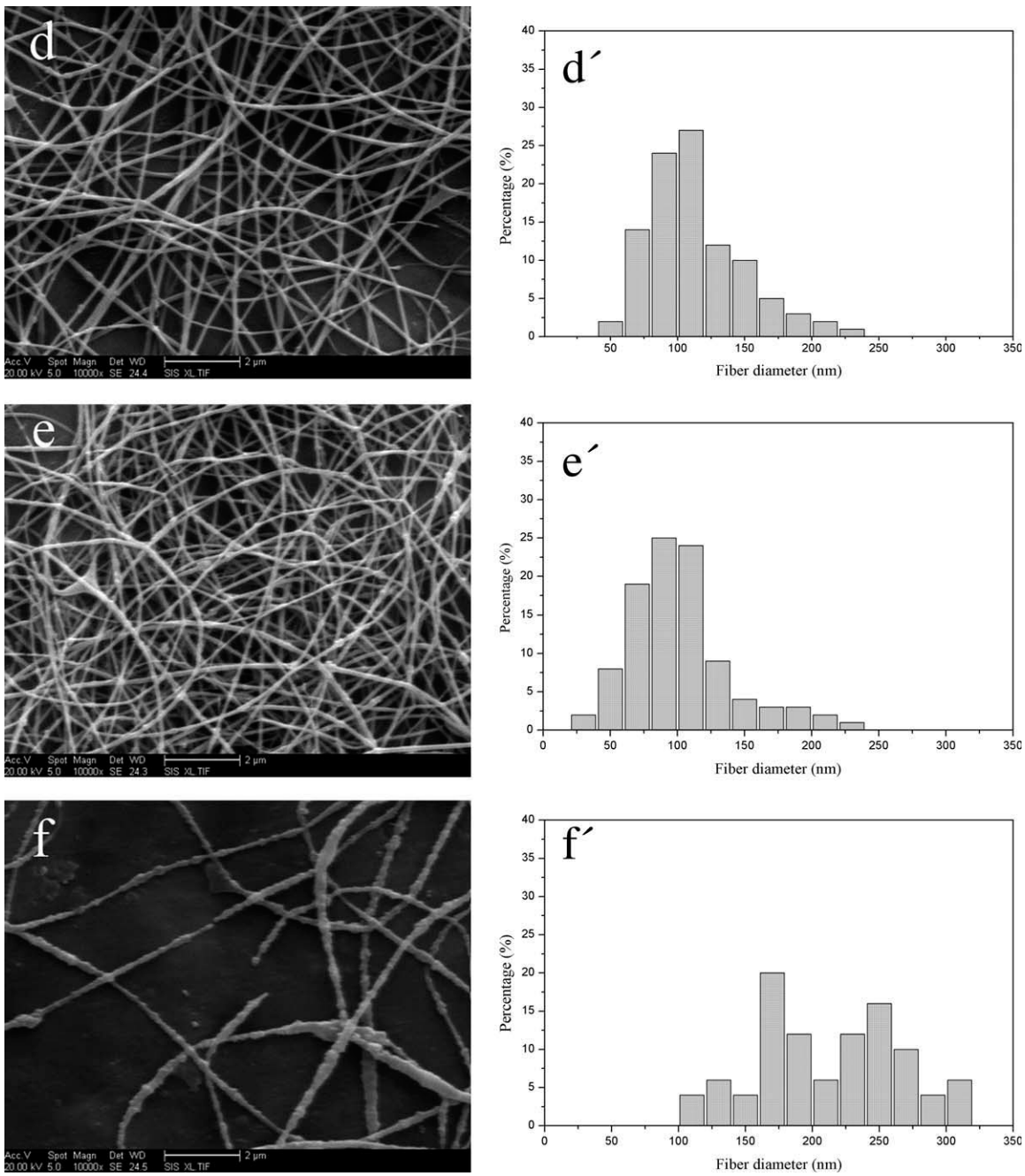

Figure 2 *(Continued from the previous page)*

RESULTS AND DISCUSSION

Morphology analysis

Figure 1 shows the SEM image of the synthesized TiO_2 nanoparticles. The average diameter of the TiO_2 nanoparticles was 40 nm, with the distribution from 10 to 60 nm. The shape of the nanoparticles was irregular.

Figure 2 shows the SEM images of the electrospun composite nanofibers with different TiO_2 content. Pure PPV nanofibers were uniform and smooth, and their average diameter was about 170 nm, with the distribution from 120 to 200 nm. PPV/TiO_2 composite nanofibers presented irregularity and relatively wide fiber diameter distribution. In addition, when the TiO_2 content increased from 0 to 18 wt %, the average fiber diameter decreased gradually from 170 to 103 nm. Conversely, in the range of 24–45 wt %, the average fiber diameter increased from 112 to 192 nm. The surface of the composite nanofibers became rough especially when TiO_2 content reached 45 wt %, and

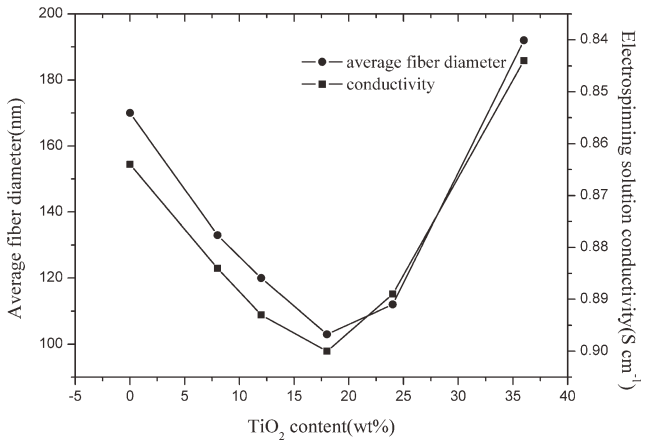

Figure 3 Average diameter of as-prepared PPV/TiO_2 composite nanofibers and conductivity of spinning solutions as a function of TiO_2 content.

some fibers appeared fibrous fracture, as shown in Figure 2(f).

Figure 3 shows the correlation between the average diameter of PPV/TiO_2 composite nanofibers and the electrical conductivity of the spinning solutions. It can be clearly seen that the changing trend of the electrical conductivity was similar to that of the average fiber diameter. It has been reported that when the solution electrical conductivity increased, there was a significant decrease in the diameter of the electrospun nanofibers.[22] High conductivity resulted in sufficient elongation of a jet by electrical force, consequently produced thinner fibers. In the same way, low conductivity meant low surface charge density, which led to the production of uniform fiber; formation of beads was also observed. When the TiO_2 content was above 18 wt %, the conductivity began to decrease. It can be explained that the aggregation of the TiO_2 nanoparticles led to two-phase separation of both polymer and inorganic particles, which had a negative effect on the conductivity.

The internal morphology and the particles dispersion of the composites were investigated by TEM, presented in Figure 4. It can be clearly seen that the TiO_2 nanoparticles were basically uniformly dispersed in the PPV nanofibers, and the particles size was heterogeneous. The particles were well dispersed individually within the nanofibers at 18 wt % TiO_2 content. The TiO_2 nanoparticles began to aggregate severely when the content was high (24 wt %). Smooth nanofibers were observed when the TiO_2 content was below 18 wt % [see Fig. 4(a–c)], and the surface of fibers became rough when the TiO_2 content was higher than 24 wt % [see Fig. 4(d,e)], due to the presence of TiO_2 nanoparticles on the fibers' surface. It was concluded that the TiO_2 nanoparticles were well dispersed in the PPV solution when the content was moderate.

The fluorescence spectra and photographs

Figure 5 shows the PL spectra of the as-spun nanofibers. It was obvious that pure PPV nanofibers showed two emission peaks at 513 and 544 nm, which belonged to the band gap of the π–π* transition and the self-absorption function of the PPV structures. For the PPV/TiO_2 composite nanofibers, the main band was almost unchanged but the peak in 513 nm had slightly blue shifted (from 513 to 510 nm) and showed a relatively wide emission band. It was also clearly that an increase in intensity of 510 nm became the dominant emission band as the TiO_2 content increased. The enhancement of this band was observed in some PPV/nanoparticle composites.[23,24] When introducing nanoparticles, the polymer chains may be break up into new short segments. The high energy of the 510-nm peak may indicate that the short segments of the polymers are involved in the emission process.[23] This blueshift and change of the intensity may be also attributed to reduced reabsorption by neighboring chains of the emitted light because the thin fibers consisted of fewer polymer chains in comparison with the thick fibers and also to much fewer interchain contacts between the polymer chains.[25] Considering all the reasons together, both processes may occur in the system.

The pure PPV nanofibers were bright yellow-green, which is accordance with fluorescence photographs in Figure 6(a). The morphology of nanofibers was similar to that observed by SEM. There were also many light spots on the PPV/TiO_2 composite nanofibers. This can be explained by following reasons: first, the addition of TiO_2 particles affected the stability of electrospinning, which resulted in the formation of beads; in addition, the centralized TiO_2 nanoparticles were excited by ultraviolet light, emitting white light, as shown in the insert part of Figure 6(c).

XRD patterns

The crystalline phase evolution of the TiO_2 nanoparticles and the resulting nanofibers has been examined using XRD measurements. The TiO_2 nanoparticles and PPV precursor were heated under the same conditions. In Figure 7, the diffraction peaks of TiO_2 nanoparticles can be assigned to the diffraction planes of the anatase phase according to the standard diffraction index. The peak at $2\theta = 25.3°$ corresponded to the (101) crystal plane of anatase and the other peaks at 38.1°, 48°, and 54.5° corresponded to the (112), (200), and (211) crystal planes. The broad

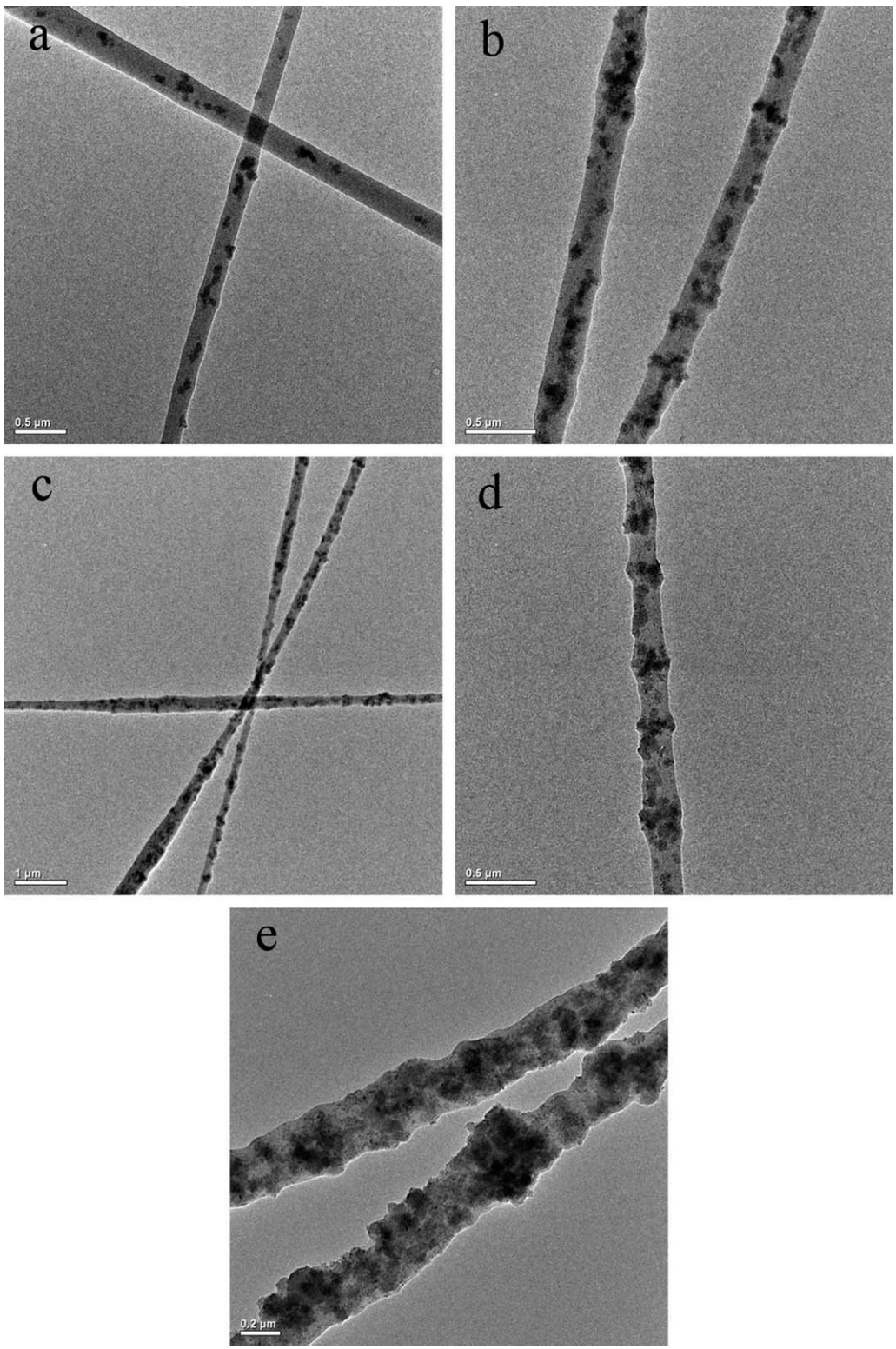

Figure 4 TEM images of PPV/TiO_2 composite nanofibers with different TiO_2 concentration: (a) 8 wt %, (b) 12 wt %, (c) 18 wt %, (d) 24 wt %, and (e) 45 wt %.

diffraction peaks were attributed to the characteristic of small particle effect.[26]

Figure 8 shows XRD patterns of pure PPV nanofibers and PPV/TiO_2 composite nanofibers with various TiO_2 content. The pure PPV nanofibers had a broad diffraction peak related to the PPV component,[27] which appeared around $2\theta = 21.2^\circ$ [see Fig. 8(a)]. The pure PPV nanofibers still kept the original

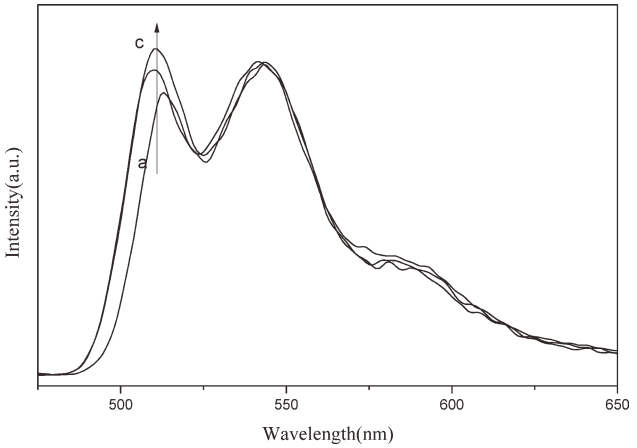

Figure 5 PL spectra of PPV/TiO_2 composite nanofibers with different TiO_2 content: (a) 0 wt %, (b) 18 wt %, and (c) 45 wt %.

crystalline region even if it was prepared by electrospinning. Seen from Figure 8(b–f), the diffraction intensity of the PPV/TiO_2 composite nanofibers was lower than that of pure PPV sample, revealing that the addition of TiO_2 nanoparticles enhanced the amorphous phase of the electrospun composite nanofibers. This can be explained that the existence of TiO_2 nanoparticles hindered the generation of crystal lattice and led to the decrease of PPV crystallinity. As can be seen from Figure 8(a–c), when the content of TiO_2 was lower than 18 wt %, there was only a broad peak belonging to PPV component. These results suggested that TiO_2 nanoparticles were indeed incorporated into PPV nanofibers. However, when the TiO_2 content was higher than 24 wt %, a weak diffraction peak appeared at 25.3°, which corresponded to the (101) crystal plane of anatase. It was indicated that when the content was high, some of the TiO_2 particles would aggregate on the surface of the nanofibers.

CONCLUSION

In this study, TiO_2 nanoparticles were synthesized by hydrolysis of precipitation of titanium alkoxide possessing the characters of the anatase TiO_2. The PPV/TiO_2 composite nanofibers containing different amount of TiO_2 nanoparticles were successfully prepared by directly mixing one-step electrospinning. The results from SEM and TEM images indicated that adulterating with different quantity of TiO_2 nanoparticles had significant influence on the nanofibers morphological characteristics such as nanofibers diameter, degree of surface roughness, and dispersion of TiO_2 nanoparticles. In addition, the PL spectra and photographs showed that short segments of the polymers and reducing reabsorption by neighboring chains may result in an increase in intensity of the high-energy shoulder, and the electrospinning process turned to be unstable when the concentration of nanoparticles increased. XRD analysis provided that the increase of TiO_2 nanoparticles

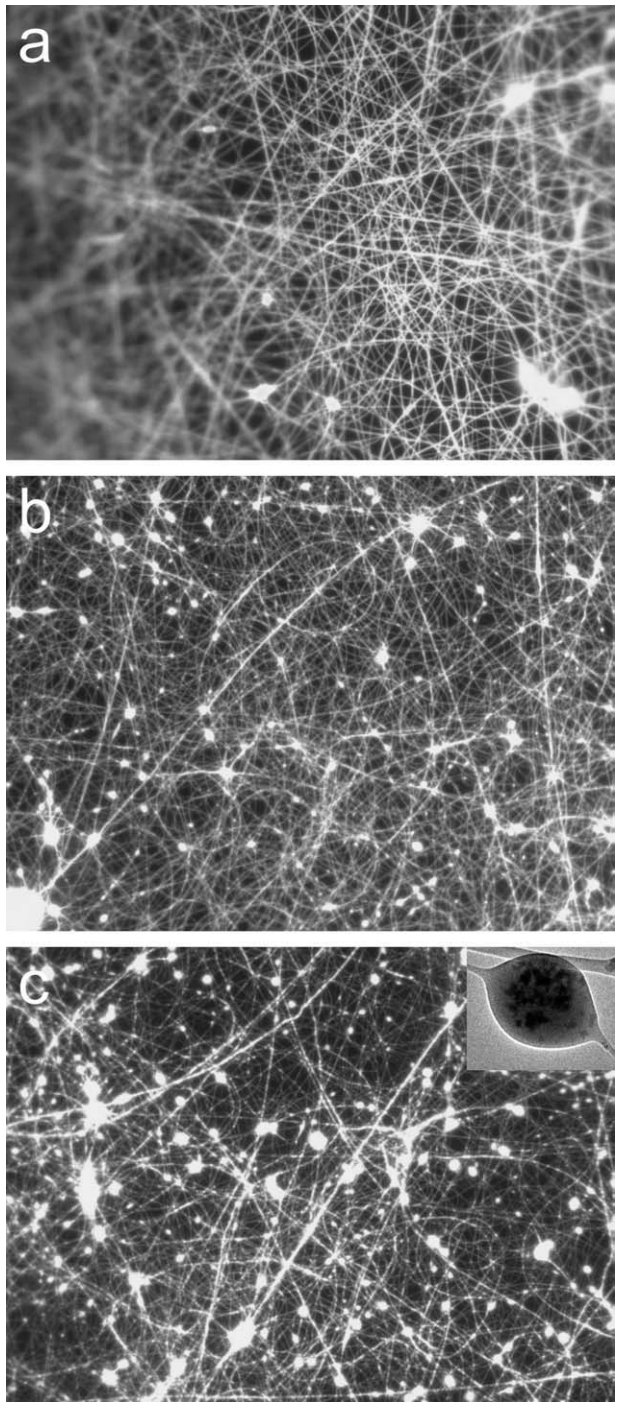

Figure 6 Fluorescence photographs of the PPV/TiO_2 composite nanofibers with different TiO_2 content: (a) 0 wt %, (b) 18 wt %, and (c) 45 wt %, inset part is a TEM image of a bead on the composite nanofibers.

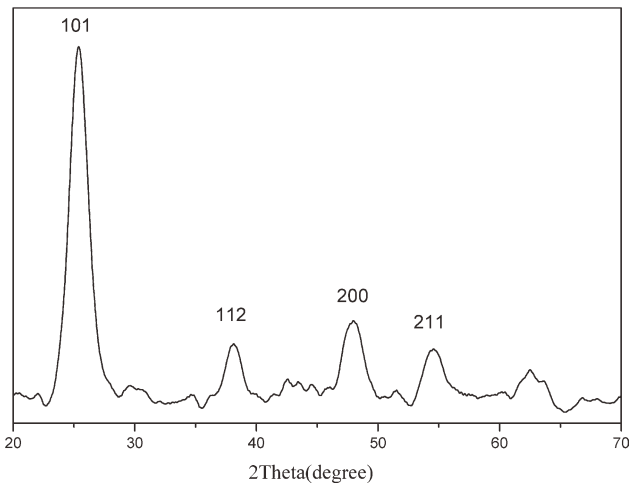

Figure 7 XRD patterns of TiO_2 nanoparticles.

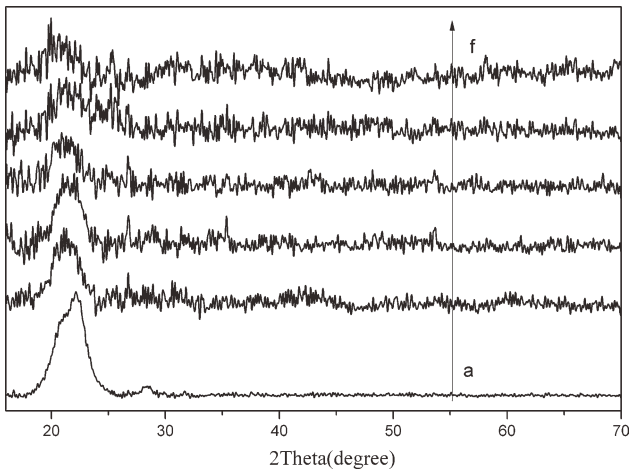

Figure 8 XRD patterns of electrospun PPV/TiO_2 composite nanofibers with various TiO_2 contents: (a) 0 wt %, (b) 12 wt %, (c) 18 wt %, (d) 24 wt %, and (e) 45 wt %.

enhanced the amorphous phase of PPV in composite nanofibers. We anticipate that this composite photoluminescent nanomaterial will have many potential applications, such as in light-emitting diodes, photocatalysts, and photocathodes.

References

1. Zhao, J. G.; Jia, C. W.; Duan, H. G.; Sun, Z. W.; Wang, X. M.; Xie, E. Q. J Alloy Compd 2008, 455, 497.
2. Chronakis, I. S. J Mater Process Technol 2005, 167, 283.
3. Reneker, D. H.; Yarin, A. L.; Fong, H.; Koombhongse, S. J Appl Phys 2000, 87, 4531.
4. Zhu, Z.; Zhang, L.; Smith, S.; Fong, H.; Sun, Y. Gosztol, D. Synth Met 2009, 159, 1454.
5. Yang, P. P.; Zhan, S. M.; Huang, Z. H.; Zhai, J. L.; Wang, D. J.; Xin, Y.; Zhang, L. J.; Sun, M.; Shao, C. Mater Lett 2011, 65, 537.
6. Xin, Y.; Huang, Z. H.; Yang, P. P.; Jiang, Z. J.; Wang, C.; Shao, C. J Appl Polym Sci 2009, 114, 1864.
7. Jiang, Z. J.; Huang, Z. H.; Yang, P. P.; Chen, J. F.; Xin, Y.; Xu, J. W. Compos Sci Technol 2008, 68, 3240.
8. Zhang, Y.; Yang, Y.; Wang, C. C.; Sun, B.; Wang, Y.; Wang, X. Y.; Shen, Q. D. J Appl Polym Sci 2008, 110, 3225.
9. Wang, C.; Yan, E. Y.; Li, G. M.; Sun, Z. Y.; Wang, S. H.; Tong, Y. B.; Li, W. W.; Xin, Y.; Huang, Z. H.; Yan, P. F. Synth Met 2010, 160, 1382.
10. Sun, H. Z.; Zhang, H.; Zhang, J. H.; Wei, H. T.; Ju, J.; Li, M. J.; Yang, B. J Mater Chem 2009, 19, 6740.
11. Lee, C. Y.; Choi, Y. J.; Park, H. H. J Appl Polym Sci 2011, 119, 811.
12. Deng, D.; Shi M. M.; Chen, F.; Jiang, X. X.; Chen H. Z. Sol Energy 2010, 84, 771.
13. Wu, J.; Coffer, J. L. J Phys Chem C 2007, 111, 16088.
14. Wang, C.; Yan, E. Y.; Huang, Z. H.; Zhao, Q.; Xin, Y. Macromol Rapid Commun 2007, 28, 205.
15. Lee, S. W.; Kim, Y. U.; Choi, S. S.; Park, T. Y.; Joo, Y. L.; Lee, S. G. Mater Lett 2007, 61, 889.
16. Wang, S. H.; Wang, C.; Zhang, B.; Sun, Z. Y.; Li, Z. Y.; Jiang, X. K.; Bai, X. D. Mater Lett 2010, 64, 9.
17. Ji, L. W.; Jung, K. H.; Medford, A. J.; Zhang, X. W. J Mater Chem 2009, 19, 4992.
18. Ji, L. W.; Zhang, X. W. Mater Lett 2008, 62, 2161.
19. He, T. S.; Zhou, Z. F.; Xu, W. B.; Ren, F. M.; Ma, H. H.; Wang, J. Polymer 2009, 50, 3031.
20. Wessling R. A. J Polym Sci: Polym Symp 1985, 72, 55.
21. Halliday, D. A. D.; Burn, P. L.; Friend, R. H.; Bradley, D. D. C.; Holmes, A. B. Synth Met 1993, 55, 902.
22. Cheng, G. H.; Yang, H.; Liang, H. D.; Ge, C. H. Rare Met Mater Eng 2010, 39, 69.
23. Ago, H.; Shaffer S. P.; Ginger, D. S.; Windle, A. H.; Friend, R. H. Phys Rev B 2000, 61, 2286.
24. Yang, S. H.; Nguyen, T. P.; Rendu, P. L.; Hsu, C. S. Compos Part A 2005, 36, 509.
25. Cimrova, V.; Neher, D. J Appl Phys 1996, 79, 3299.
26. Bhardwaj, N.; Kundu, S. C. Biotechnol Adv 2010, 28, 325.
27. Wang, M. Q.; Wang, X. G. Polymer 2008, 49, 1587.